Biodegradation (2007) 18:439–452
DOI 10.1007/s10532-006-9073-7

ORIGINAL PAPER

Thermodynamic and kinetic analysis of the H_2 threshold for *Methanobacterium bryantii* M.o.H

Fatih Karadagli · Bruce E. Rittmann

Received: 16 June 2006 / Accepted: 25 July 2006 / Published online: 8 November 2006
© Springer Science+Business Media B.V. 2006

Abstract H_2 thresholds, concentrations below which H_2 consumption by a microbial group stops, have been associated with microbial respiratory processes such as dechlorination, denitrification, sulfate reduction, and methanogenesis. Researchers have proposed that observed H_2 thresholds occur when the available Gibbs free energy is minimal ($\Delta G \approx 0$) for a specific respiratory reaction. Others suggest that microbial kinetics also may play a role in controlling the thresholds. Here, we comprehensively evaluate H_2 thresholds in light of microbial thermodynamic and kinetic principles. We show that a thermodynamic H_2 threshold for *Methanobacterium bryantii* M.o.H. is not controlled by ΔG for methane production from $H_2 + HCO_3^-$. We repeatedly attain a H_2 threshold near 0.4 nM, with a range of 0.2–1 nM, and ΔG for methanogenesis from $H_2 + HCO_3^-$ is positive, +5 to +7 kJ/mol-H_2, at the threshold in most cases. We postulate that the H_2 threshold is controlled by a separate reaction other than methane production. The electrons from H_2 oxidation are transferred to an electron sink that is a solid-phase component of the cells. We also show that a kinetic threshold (S_{min}) occurs at a theoretically computed H_2 concentration of about 2400 nM at which biomass growth shifts from positive to negative.

Keywords Hydrogen · Thresholds · *Methanobacterium bryantii* · Gibbs free energy · Microbial kinetics

F. Karadagli · B. E. Rittmann
Department of Civil and Environmental Engineering, Northwestern University, 2145 Sheridan Road, Evanston, IL 60208-3109, USA

Present Address:
F. Karadagli (✉)
School of Engineering, Department of Environmental Engineering, Sakarya University, Esentepe, Sakarya 54187, Turkey
e-mail: fkaradagli@sakarya.edu.tr

Present Address:
B. E. Rittmann
Center for Environmental Biotechnology, Biodesign Institute at Arizona State University, 1001 South McAllister Avenue, 875701, Tempe, AZ 85287-5701, USA

Introduction

In anaerobic environments, fermentative microorganisms degrade complex organic materials and produce H_2, which is consumed by various H_2-oxidizing microorganisms, including denitrifiers, iron and manganese reducers, sulfate reducers, methanogens, and dehalogenators (Zehnder 1988; Schink 1997). Because H_2 is such a common electron donor, competition for available H_2 is

keen among the H_2-oxidizing microorganisms (Lovley et al. 1982; Lovley and Klug 1983; Robinson and Tiedje 1984). Experimental studies on competition suggest that each terminal electron-accepting process, i.e., denitrification, Fe(III) and Mn(IV) reduction, or sulfate reduction, has a unique hydrogen concentration associated with it. This unique H_2 concentration, called the H_2 threshold, is considered an indicator of that particular metabolic activity, e.g., sulfate reduction (Shrout et al. 2005; Kassenga et al. 2004; Lu et al. 2004; Luijten et al. 2004; Kotsyurbenko et al. 2001; Mazur and Jones 2001; Löffler et al. 1999; Krumholz et al. 1999; Hoehler et al. 1998; Yang and McCarty 1998; Löffler et al. 1997; Chapelle et al. 1996; Lovley et al. 1994; Klüber and Conrad 1993; Häring and Conrad 1991; Conrad and Wetter 1990; Cord-Ruwisch et al. 1988; Lovley and Goodwin 1988; Lee and Zinder 1988; Lovley 1985; Conrad et al. 1983; Lovley et al. 1983 and 1982.)

In a general sense, a threshold is defined as the minimum concentration below which the substrate is not scavenged (Lovley 1985; Widdel 1988; Conrad 1996). Tiedje (1988) indicated that a threshold implies a critical value for a breakpoint from one process to another, e.g., minimum oxygen levels to switch from aerobiosis to denitrification. In the context of thermodynamics, Zinder (1993) defined a threshold as the minimum concentration of a reactant, e.g., H_2, to allow a specific reaction to be thermodynamically favorable based on the Gibbs free energy relationship.

Many researchers suggest that H_2 thresholds depend on the free-energy yield of the respiratory reaction and the physiological characteristics of the H_2-consuming microorganisms (Lovley and Goodwin 1988; Conrad and Wetter 1990; Hoehler et al. 1998; Zinder 1993; Brown et al. 2005). H_2 thresholds have been measured for pure or mixed cultures in various systems, e.g., batch reactors (Conrad et al. 1983; Lovley 1983; Cord-Ruwisch 1988; Conrad and Wetter 1990; Häring and Conrad 1991; Klüber and Conrad 1993; Löffler et al. 1997, 1999; Krumholz et al. 1999; Mazur and Jones 2001; Luijten et al. 2004), completely mixed reactors (Yang and McCarty 1998), sediments (Lovley et al. 1982 and 1983; Hoehler et al. 1998; Mazur and Jones 2001), constructed wetlands (Kassanga et al. 2004), and aquifers (Lovley and Goodwin 1988; Lovley et al. 1994; Chapelle et al. 1996; Luijten et al. 2004), and researchers suggest that H_2 thresholds follow a thermodynamically controlled trend that is homoacetogenesis > methanogenesis > sulfate reduction > iron reduction > nitrate reduction (Lovley and Goodwin 1988; Lovley et al. 1994; Chapelle et al. 1996; Hoehler et al. 1998; Brown et al. 2005). This trend is in the same direction as the standard Gibbs free energies ($\Delta G°$) of these metabolic reactions; therefore, it has been proposed that H_2 thresholds can be computed using the Gibbs free energy equation (Lovley and Goodwin 1988; Lee and Zinder 1988; Conrad and Wetter 1990; Kotsyurbenko et al. 2001; Conrad 1996). When several researchers calculated the Gibbs free energy (ΔG) at their observed H_2 threshold, they obtained a small negative free energy, and they attributed this energy as the critical minimal energy necessary for microbial survival (Conrad and Wetter 1990; Lu et al. 2004; Seitz et al. 1988). Similarly, other researchers observed in syntrophic co-cultures of fermenting and methanogenic bacteria that at least –15 to –35 kJ/mol-reaction of free energy was necessary for production or consumption of H_2 (Schink 1997; Seitz et al. 1988). On the other hand, Jackson and McInerney (2001) observed that syntrophic reactions of fermenting and sulfate-reducing or methanogenic bacteria can proceed until the absolute thermodynamic limit is observed.

In addition to thermodynamics, several studies suggest that microbial kinetic parameters, such as H_2-consumption rate, specific growth rate, and biomass decay rate, also may play a role in controlling H_2 thresholds (Lovley et al. 1982, 1983; Robinson and Tiedje 1984; Lovley 1985; Lovley and Goodwin 1988; Brown et al. 2005). Lovley and Goodwin (1988) proposed that H_2 consumption depends on the kinetic parameters of the microorganisms consuming H_2; therefore, each predominant H_2-consuming process should have a characteristic H_2 concentration, which can be the H_2 threshold for that particular microbial process.

In this study, we comprehensively test how thermodynamics and microbial kinetics control

H_2 thresholds. We first provide mechanistic definitions and computation methods for distinct types of thresholds. To evaluate theoretical and observed experimental thresholds, we carry out an experimental program using methanogenesis as the respiratory reaction and *Methanobacterium bryantii* M.o.H. as a model methanogen that uses H_2 as its sole electron donor.

Theoretical basis

Methanogenesis is the ideal system for studying H_2 thresholds for several reasons. First, available is *Methanobacterium bryantii* M.o.H., a well-described methanogen that uses only H_2 as its electron donor and can be obtained as a pure culture from Deutsche Sammlung von Mikroorganismen und ZellKulturen GmbH (DSMZ) (www.dsmz.de) (Culture Number: 863) (Benstead et al. 1991). *M. bryantii* cells are long rods with blunt round ends—0.5–1 μm in width, and 10–15 μm in length—that can easily be detected by simple light microscopy, which is an advantage for monitoring growth and purity of the microbial culture (Boone 1987; Boone and Mah 1989), as we did regularly in this study. Second, the biochemistry and enzymology of CH_4 production from H_2 and CO_2 are well studied (Zinder 1993; Deppenmeier 2002; Thauer 1998), making possible mechanistic interpretations of experimental results. Finally, a significant number of H_2 thresholds is reported for methanogens (Lovley 1985; Cord-Ruwisch et al. 1988; Lovley and Goodwin 1988; Conrad and Wetter 1990; Hoehler et al. 1998) and for *M. bryantii* M.o.H. (Lovley 1985), allowing us to compare our results with those from previous studies.

In thermodynamics, the Gibbs free energy assesses the feasibility of a reaction. A negative Gibbs free energy for a reaction means that the reaction can proceed in the proposed direction. For methanogenesis with H_2, the reaction and the Gibbs free-energy equation are

$$0.25\,HCO_3^- + H_{2(aq)} + 0.25\,H^+ \rightarrow 0.25\,CH_{4(aq)} + 0.75\,H_2O_{(1)} \quad (1)$$

$$\Delta G = \Delta G^o + R * T * \ln \frac{\{CH_{4(aq)}\}^{0.25} * \{H_2O_{(l)}\}^{0.75}}{\{HCO_3^-\}^{0.25} * \{H_{2(aq)}\} * \{H^+\}^{0.25}} \quad (2)$$

where {..} indicates activities in liquid phase, T is temperature (K), R is the ideal gas constant (L-atm/mol-K), $\Delta G°$ is the standard Gibbs free energy of the reaction (kJ/mol-H_2), and ΔG is the net free energy of the reaction for a given experimental condition. We computed $\Delta G° = -57.3$ kJ/mol-H_2 using the following $\Delta G_f°$ values in kJ/mol from (Stumm and Morgan 1996; Dolfing and Janssen 1994; Rittmann and McCarty 2001); $H_{2(aq)} = 17.57$; $HCO_{3(aq)}^- = -586.8$; $H^+_{(aq)} = 0$; $CH_{4(aq)} = -34.39$; $H_2O_{(l)} = -237.18$. The reaction is thermodynamically feasible if $\Delta G < 0$. The minimum H_2 activity that will make methanogenesis feasible—in other words, the strict-thermodynamic threshold for methanogenesis—is computed by making $\Delta G = 0$ and solving above equation for $\{H_{2(aq)}\}$.

$$\{H_{2(aq)}\}_{threshold} = \frac{\{CH_{4(aq)}\}^{0.25}}{\{HCO_3^-\}^{0.25} * \{H^+\}^{0.25} * e^{(\Delta G°/R*T)}} \quad (3)$$

A H_2 activity greater than the threshold makes $\Delta G < 0$ and, thus, methanogenesis from H_2 thermodynamically feasible. According to Eq. 3, the value of the strict-thermodynamic threshold depends on the activities of methane, bicarbonate, and H^+. In our work, all experiments were conducted in DSMZ Medium #119, in which pH was fixed at 7.2 with the carbonate buffer and the bicarbonate activity was 0.03, a value much higher than the activities of all other reactants and products; thus, the change in HCO_3^- activity was negligible for our experiments. Consequently, only the methane activity controlled the strict-thermodynamic threshold for H_2.

In the context of microbial kinetics, a kinetic threshold is the minimum substrate concentration that balances microbial growth and decay (Rittmann and McCarty 1980a, b; Lovley and Goodwin 1988; Rittmann and McCarty 2001; Brown et al. 2005). In particular, the kinetic

threshold (S_{min}) is defined as the minimum substrate concentration required by cells to synthesize new biomass that replaces biomass loss, e.g., through endogenous respiration, lysis of the cell membrane, physical detachment, or predation (Rittmann and McCarty 2001). S_{min} can be estimated from Monod kinetics (Rittmann and McCarty 2001; Monod 1949) applied to a batch reactor:

$$\frac{dX_a}{dt} = \left[\mu_{max} * \left(\frac{S}{Ks + S}\right) - b\right] * X_a = \left[Y * q_{max} * \left(\frac{S}{Ks + S}\right) - b\right] * X_a \quad (4)$$

where X_a is the active biomass (mass-cell/ volume), μ_{max} is the maximum specific growth rate of the population (1/time), S is the concentration (mass/volume) of the growth-rate limiting substrate, Ks is the Monod-half-maximum-rate concentration (mass-substrate/volume), Y is the true yield or the mass of cells produced per unit mass of substrate consumed (mass-cell/mass-substrate), q_{max} is the maximum substrate consumption rate per time (mass-substrate/mass-cell/time), and b is the first-order decay rate (1/time). At steady-state, the rate of change in active biomass (dX_a/dt) is zero, and we solve for S_{min} as

$$S_{min} = \frac{b * Ks}{(\mu_{max} - b)} = \frac{b * Ks}{(Y * q_{max} - b)} \quad (5)$$

If the H_2 concentration is less than S_{min}, steady-state biomass cannot be maintained, and biomass that is present decays away, or has a net negative growth rate. S_{min} has been well studied in the past (e.g., Rittmann and McCarty 1980a, b; Namkung and Rittmann 1987), but its relation to observed H_2 thresholds has been hardly investigated (Lovley and Goodwin 1988; Brown et al. 2005).

We performed a series of batch experiments to determine if kinetic and thermodynamic H_2 thresholds were reproducible and if the thermodynamic threshold depended on the methane activity, as indicated by Eq. 3. We computed the kinetic threshold for *M. bryantii* M.o.H. (c. 2400 nM) from our experimentally obtained values of Monod kinetic parameters (Karadagli and Rittmann, 2005): μ_{max} = 0.77 /day; Ks = 18000 nM; and b = 0.09/day. For each experiment, we estimated the thermodynamic H_2 threshold using experimental activities for HCO_3^-, H^+, and CH_4. Our experimental results show that the kinetic (S_{min}) threshold and another threshold exist and are reproducible. Although the experimental kinetic threshold corresponds to the theoretical S_{min} value, the second threshold does not follow thermodynamics of methanogenesis as indicated by Eq. 3. We repeatedly attained a H_2 threshold for *M. bryantii* M.o.H. (c. 0.4 nM) that gave positive ΔG for methanogenesis from H_2, which means that H_2 oxidation cannot be coupled with methane formation at the H_2 threshold. Instead, H_2 oxidation must be coupled to another reaction.

Experimental methods

We obtained *M. bryantii* M.o.H. as a living-culture from Deutsche Sammlung von Mikroorganismen und ZellKulturen GmbH (DSMZ #863). We grew *M. bryantii* cultures in DSMZ medium#119 for *M. bryantii* and conducted threshold experiments with microorganisms harvested from exponential growth phase. We transferred the source culture from DSMZ into 5 growth tubes and observed growth in all tubes under a headspace atmosphere of 80% CO_2 + 20% H_2. We continually transferred the culture into new growth tubes and maintained a living culture throughout the experiments. We routinely conducted microscopic examination of the culture to ensure that only the unique *M. bryantii* M.o.H. cells were present; no contaminating cells were found in any instance.

We computed the bicarbonate concentration from the medium composition and measured pH (= 7.2). To compute ΔG, we converted concentrations to activities using activity coefficients computed with Davies and the extended Debye-Hückel equations (Stumm and Morgan, 1996) for the ionic strength of the medium, I = 0.123. The extended Debye-Hückel equation considers ion size; therefore the activity coefficients for HCO_3^- (ion size 4 Å) and H^+ (ion size 9 Å) were 0.77 and 0.81, respectively. In contrast, the Davies

equation, which does not consider ion size, gave 0.76 for a general group of all mono-valent ions in the system. We used 0.77 and 0.81 for HCO_3^- and H^+, respectively. We estimated the activity corrections for dissolved gases using the salting-out equation—log(activity coefficient) = k_s*I—where k_s is the salting-out coefficient, and its value is usually 0.1 (Stumm and Morgan 1996). The activity coefficient for all gases was 1.03.

We conducted threshold experiments in 28-ml anaerobic tubes filled with 5 or 10 ml of liquid media (Ljungdahl et al. 1986). The tubes were kept horizontal in a shaker-incubator rotating at 200 rpm with inside temperature at 37°C. The tubes were exposed to room temperature (22–23°C) for 15–20 min during sampling. We conducted a total of 21 independent experiments, including duplicate and triplicate tubes that yielded similar H_2 thresholds. In all of the experiments, we made comprehensive measurements of H_2, CH_4, and biomass. To obtain desired initial H_2 concentrations, we aseptically added 80% H_2 + 20% CO_2 gas mixture to the desired total pressure, e.g., 0.1 to 0.8 atm, and then adjusted the total pressure inside the tube to 1 atm with 80% N_2 + 20% CO_2 or 100% N_2 (Ljungdahl et al. 1986). We monitored consumption of H_2 and production of CH_4 by taking gas samples with gas-tight syringes. Duplicate gas samples were removed from each tube, while triplicate samples were taken at various points in each experiment. The gas samples (0.1–1 ml) were placed into dilution bottles of the following sizes (240 ml, 140 ml, 9 ml) and analyzed immediately. Prior to receiving gas samples, dilution bottles were capped with blue rubber stoppers and flushed with pure N_2 until the background H_2 in the bottles was undetectable (H_2 < 0.05 ppm or 0.04 nM). Gas samples were not diluted for H_2 when H_2 concentration in the growth tubes were less than 10 nM, the maximum point of our H_2-calibration curves. We used commercial H_2 standards from Air Products Inc. (20 ppm in N_2, equivalent to an aqueous-phase concentration of 15 nM) and prepared two ranges of calibration curves for H_2 measurements, (0.1–0.9) nM and (1–10) nM. Based on standards, H_2 had a linear response above 0.05 nM.

We analyzed the samples for CH_4 and H_2 with gas chromatography (GC) and a reduction gas analyzer (RGA), respectively. The GC was a Hewlett-Packard 5890 series II, equipped with Porapak Q column (80/100, $6' \times 1/8''$SS) and operated with temperatures of 70, 60, and 80°C for injector, column, and detector, respectively. For the GC, the carrier gas, fuel, and air were research-grade N_2 at flow rate of 35 ml/min, research-grade H_2 at 50 ml/min, and air at flow rate of 470 ml/min, respectively. The RGA was a RGA III from Trace Analytical, Inc. (Palo Alto, California). We operated the RGA at column temperature of 104°C and detector temperature of 265°C. Each gas sample was injected into the GC or RGA at least two and mostly three times, and the average readings are reported.

The liquid-phase H_2 and CH_4 concentrations were computed from the gas-phase measurements using Henry's Law by assuming equilibrium between gas and liquid phases. We searched the literature for Henry's law constants for H_2 and CH_4 and used $7.8*10^{-4}$ mol/l-atm for H_2 and $1.4*10^{-3}$ mol/l-atm for CH_4 at 25°C. We corrected these values for 37°C using the van't Hoff equation (Stumm and Morgan 1996), yielding $7.3*10^{-4}$ and $1.12*10^{-3}$ mol/l-atm for H_2 and CH_4, respectively. Although the detection limit for RGA was around 0.01 ppm (0.008 nM), interferences from the carrier gas, which had 0.05 ppm H_2, allowed us to measure H_2 reliably down to 0.1 ppm (corresponding to ~ 0.08 nM in the aqueous phase). Thus, the detection limit for H_2 was 0.05 ppm, and the quantification limit was 0.1 ppm in the gas phase. The reproducibility of H_2 measurements was 2–3%, while it was 4–5% for methane. We prepared control tubes with no biomass added, and the H_2 concentration remained constant for up to 100 days until this experiment was terminated.

Biomass concentrations were measured with a spectrophotometer using optical density units (O.D.) at 600 nm wavelength and via a modified version of Bradford protein assay (Mägli et al. 1995). The correlation between O.D. values and protein measurements was linear as indicated with: (mg protein/l) = 71.344*(O.D.) + 1.494 (R^2 = 1.00). Reproducibility of O. D. values was 2–3%.

Table 1 Summary of experimental conditions and results for all experiments in this study

Initial OD_{600}	Initial $\{H_2\}_{liq}$ (nM)	Initial $\{CH_4\}_{liq}$ (nM)	Final $\{CH_4\}_{liq}$ (nM)	Computed H_2 threshold[a] (nM)	Observed H_2 threshold (nM)	ΔG^b (kJ/mol-H_2)
0.2	747,000	50,000	330,000	4.4	0.35–0.5	+7
0.045	431,000	304,107	440,000	4.9	0.4	+6
0.3	375,000	247,393	390,000	4.8	0.35	+5
0.01	213,000	837	74,000	3.1	0.35–0.5	+4
0.065	197,000	53300	120,000	3.6	0.35–0.7	+4
0.007	32,400	987	11,000	1.9	0.4–0.6	~ + 2
0.01	16,400	753	7,000	1.7	0.4–0.8	~0
0.016	110	3	30	0.4	0.7–0.8	–3
0.008	55	5	39	0.4	0.6–1.0	–2
0.24	0.5	45	4800	1.5	0.4	~0

[a] Computed strict-thermodynamic H_2 threshold

[b] ΔG for methanogenesis when H_2 oxidation stopped

Results

Table 1 summarizes the conditions for ten experiments in which we comprehensively measured H_2, CH_4, and biomass, thereby providing the complete relationships among H_2 utilization, CH_4 production, and growth or decay of biomass. In total, we ran 21 independent experiments that showed the same patterns of H_2 consumption and threshold. Here, we present ten experimental results that illustrate all features of our findings. The rest of the threshold experiments are duplicates or triplicates of the experiments in Table 1. We used initial H_2 concentrations ranging from 55 nM to 747,000 nM, and these gave final CH_4 concentrations that ranged from 30 nM to 440,000 nM. In a few experiments, we aseptically added methane to the tubes; in these cases, the final methane concentration was much higher than the stoichiometric molar ratio for H_2:CH_4 of 4:1 (Eq. 1). The strict-thermodynamic H_2 thresholds, computed by Eq. 3, ranged from 0.38 to 4.9 nM, with the higher values corresponding to the higher final CH_4 concentrations.

We obtained the same patterns in all experiments, including biomass decay after the H_2 concentration dropped below S_{min}, a reproducible H_2 threshold around 0.4 nM (with a range of 0.2–1 nM), and cessation of CH_4 generation before the H_2 threshold. Figs. 1–4 illustrate the detailed results for four experiments that clearly highlight the key trends observed in all experiments.

Figure 1 shows the results from the experiment that had the initial H_2 concentration of 431,000 nM. We aseptically added about 300,000 nM CH_4 to this tube prior to the experiment, and, with methane generated due consumption of H_2, the final CH_4 concentration was 440,000 nM, which gave a strict-thermodynamic threshold of 4.9 nM. The observed H_2 threshold, however, was around 0.4 nM, a value approximately 12 times lower than the computed threshold. Although ΔG was negative up to the cessation of methane generation (i.e., up to 3 days), ΔG became positive (+5 to +7 kJ/mol-H_2) by the time H_2 oxidation stopped.

The kinetic threshold, S_{min}, occurred between 1.5 and 2 days, when the biomass growth rate changed from positive to negative. As indicated by Eq. 4, a substrate concentration less than S_{min} makes biomass growth smaller than biomass decay, and biomass concentration must decline over time. The H_2 concentration during this transition period was in the range of 5,000–1,000 nM, which brackets the estimated S_{min} of 2400 nM.

Figure 2 shows the results from an experiment with an initial H_2 concentration of 196,600 nM and a final CH_4 concentration of 120,000 nM. The computed strict-thermodynamic threshold was 3.6 nM. Figure 2a shows that most of the H_2 was consumed over 2 days, and a threshold plateau of H_2 (0.35–0.7 nM) was observed from day 2 to day 8, when the experiment was terminated. The H_2 threshold was 5–10 times smaller than the theoretical strict-thermodynamic threshold (3.6 nM). Consequently, ΔG for methanogenesis was positive, up to +5 to +6 kJ/mol-H_2 (Fig. 2b). CH_4 production stopped before the time that ΔG became positive. S_{min} occurred at 1.4 days, when the biomass growth rate changed from positive to

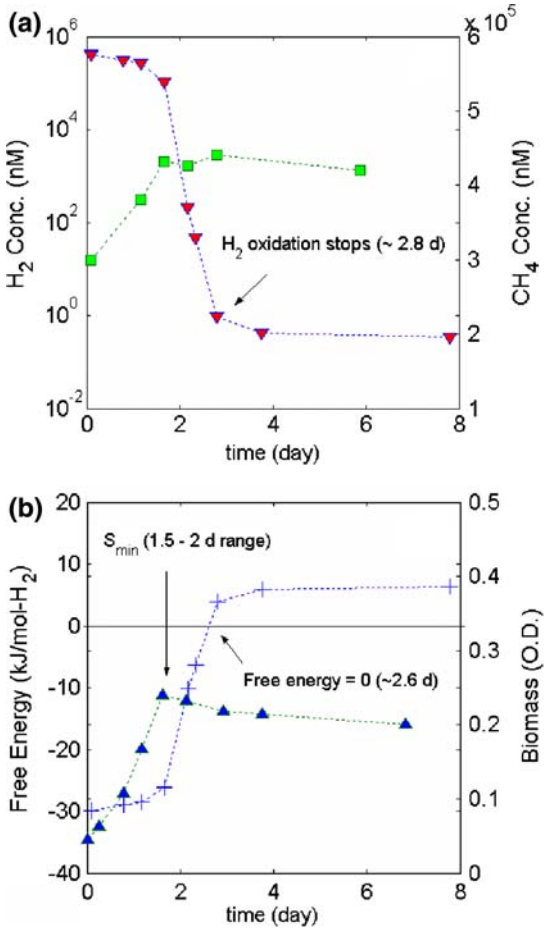

Fig. 1 Experimental results from H_2 threshold experiments with *M. bryantii* M.o.H. when the initial H_2 concentration was 431,000 nM and the final CH_4 concentration was 440,000 nM: (**a**) Liquid phase H_2 (downward triangles) and CH_4 (squares), y-axis is logarithmic, (**b**) Free energy (+) and biomass concentration as O.D. (triangles)

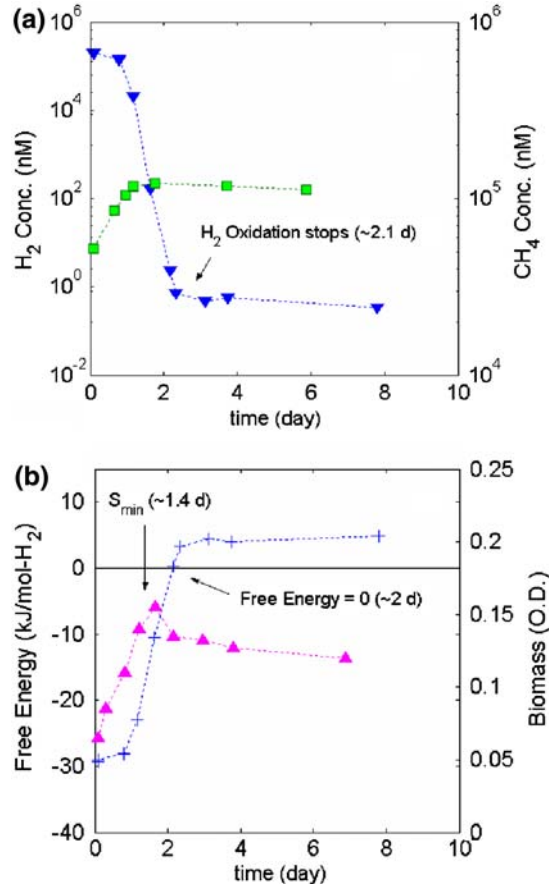

Fig. 2 Experimental results from H_2 threshold experiments with *M. bryantii* M.o.H. when the initial H_2 concentration was 196,600 nM and the final CH_4 concentration was 120,000 nM: (**a**) Liquid phase H_2 (downward triangles) and CH_4 (squares), y-axis is logarithmic, (**b**) Free energy (+) and biomass concentration as O.D. (triangles)

negative. At the peak of the biomass curve (i.e., S_{min}), the H_2 concentration was approximately 2400 nM.

Figure 3 shows the results from the experiment with a lower initial H_2 concentration, 32,400 nM. The final CH_4 concentration of 11,000 nM was generated by consumption of only the initial H_2, as we added no methane prior to the experiment. Though the computed strict thermodynamic threshold was 1.9 nM, H_2 consumption continued below this value, down to 0.6 nM at around 4 days. CH_4 generation leveled off around the time that ΔG was no longer negative. The H_2 concentration declined to around 0.4 nM on day 28, giving a final ΔG of ~ +2 kJ/mol-H_2 for methanogenesis. S_{min}, again near 2400 nM, occurred around 1.5 days (Fig. 3b).

Figure 4 presents the results from an experiment in which we stripped out all H_2 and CH_4 before adding a very small initial H_2 concentration, 55 nM. The final CH_4 concentration was 39 nM, giving a computed strict thermodynamic threshold of 0.4 nM. The observed threshold was 0.6–1.0 nM. Because the final H_2 concentration was above the computed theoretical threshold, although in the same range as in the other experiments, the final ΔG was slightly negative (–2 kJ/mol H_2). CH_4 generation stopped at the

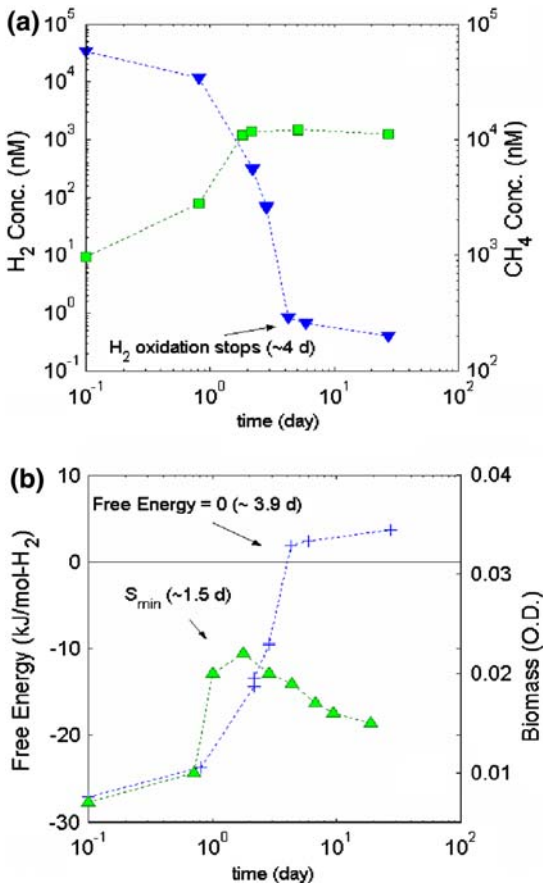

Fig. 3 Experimental results from H_2 threshold experiments with *M. bryantii* M.o.H. when the initial H_2 concentration was 32,400 nM and the final CH_4 concentration was 11,000 nM: (**a**) Liquid phase H_2 (downward triangles) and CH_4 (squares), y-axis is logarithmic, (**b**) Free energy (+) and biomass concentration as O.D. (triangles)

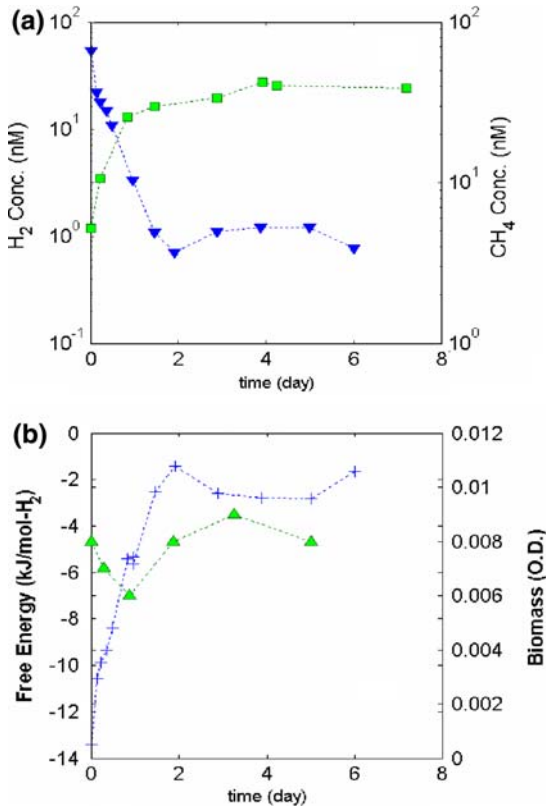

Fig. 4 Experimental results from H_2 threshold experiments with *M. bryantii* M.o.H. when the initial H_2 concentration was only 55 nM and the final CH_4 concentration was 43 nM: (**a**) Liquid phase H_2 (downward triangles) and CH_4 (squares), y-axis is logarithmic, (**b**) Free energy (+) and biomass concentration as O.D. (triangles)

time that H_2 oxidation stopped. The initial H_2 concentration was below the S_{min} concentration; thus, biomass showed no clear-cut growth and decay phases.

Figure 5 shows that starved *M. bryantii* cells oxidized the small amount of initial H_2, while not producing methane, indicating that the cells transferred electrons to an electron sink other than CH_4. In parallel with Fig. 4, sequential additions of H_2 at initial concentrations of 155 and 340 nM were consumed to the same threshold of 0.2–0.4 nM. Starved *M. bryantii* cells did not oxidize CH_4 when its concentration was 52 nM or 488,000 nM (approximately ~50% of the headspace gas mixture) during the first and second injections of H_2, respectively. Pressurized control tubes having no *M. bryantii*, but the normal medium, showed no decrease in H_2 concentration, meaning that all observed H_2 oxidation was catalyzed by *M. byrantii*.

Figure 6 shows that biomass served as an electron donor for the production of CH_4 and H_2 if the concentrations of H_2 and CH_4 were decreased suddenly for rapidly growing *M. bryantii* M.o.H. by stripping out the gases by purging with N_2 gas. Rapidly growing cells (i.e., positive growth before reaching S_{min}) were able to generate CH_4 and H_2 rapidly from biomass when the thermodynamics for those reactions were made favorable by removal of each reduced gas. Ultimately, the produced H_2 was oxidized, and its

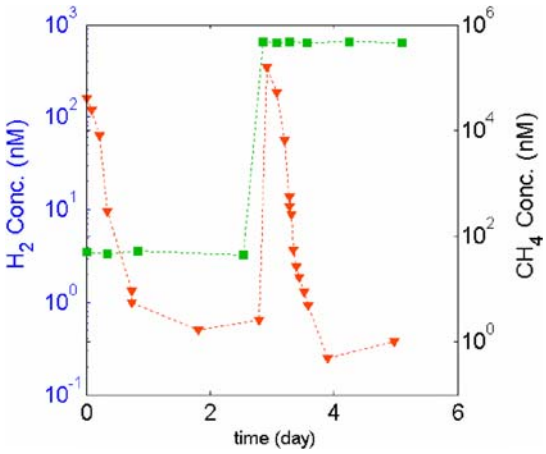

Fig. 5 H_2 (downward triangles) and CH_4 (squares) concentrations during H_2 addition-experiment to starved *M. bryantii* M.o.H cells, when O.D. = 0.18. For the second addition of H_2, the CH_4 concentration was increased from an average of 52 nM to an average of 488,000 nM (~50% in the head space) by aseptic addition of CH_4. Y-axes are logarithmic with different scales

concentration driven to the same ~0.4-nM level as for when H_2 was provided exogenously.

Table 1 summarizes the threshold values and final ΔG values for all experiments, including those not presented graphically. The combined results from all experiments show consistent patterns. First, S_{min} reliably occurred around 2400 nM, when the biomass net growth rate became negative. Our kinetic threshold value is also supported by a recent study of Brown et al. (2005), who observed S_{min} = 1300 nM for methanogens. Second, CH_4 generation stopped before ΔG for methanogenesis went from negative to positive. Laws of thermodynamics disallow methane generation when its $\Delta G > 0$, and the experimental results are consistent with this thermodynamic requirement. Third, the H_2 concentration at which H_2 oxidation by *M. bryantii* M.o.H. stopped was consistently near 0.4 nM (range of 0.2–1 nM) and had a positive ΔG for methanogenesis in most cases. Thus, the H_2 thermodynamic threshold was not controlled by ΔG of methanogenesis from H_2 and HCO_3^- (Table 1), and the electrons from H_2 oxidation had to have gone to another electron sink.

To further evaluate the strength of the conclusion that ΔG was positive at the thermodynamic threshold, we computed the maximum possible ranges of ΔG at the threshold based on the average 5% uncertainty in the H_2 and CH_4 activities. The ranges of ΔG values were small: 6.68 ± 0.2, 5.48 ± 0.19, 2.80 ± 0.16, and –2.41 ± 0.28 kJ/mol-H_2 for the results in Figs. 1, 2, 3, and 4, respectively.

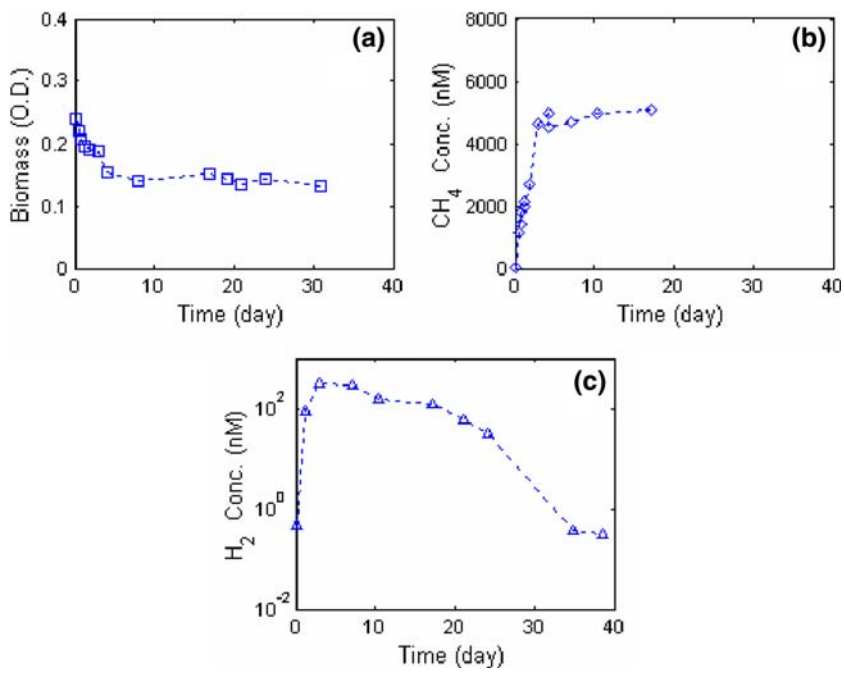

Fig. 6 Effects of removing H_2 and CH_4 from rapidly growing *M. bryantii* M.o.H. by purging the culture tube with N_2 (or $N_2 + CO_2$). Biomass concentration (**a**) continually decayed with no exogenous H_2 source. Endogenous electron donor gave initial CH_4 (**b**) and H_2 (**c**) productions. Ultimately, the H_2 concentration declined to ~0.4 nM

Clearly, most of the ΔG values were positive at the threshold. Furthermore, using 50% uncertainty in the H_2 and CH_4 measurements still maintained the positive ΔG ranges at the thresholds. Thus, the conclusion that ΔG for methanogenesis was repeatedly positive is robust.

Discussion

The H_2 thresholds previously reported for methanogens range from 6 nM to 77 nM (Yang and McCarty 1998; Lovley 1985; Cord-Ruwisch et al. 1988; Lovley and Goodwin 1988; Lee and Zinder 1989; Lovley et al. 1994; Löffler et al. 1997 and 1999; Luijten et al. 2004; Kotsyurbenko et al. 2001; Lu et al. 2004). The reported H_2 thresholds for *M. bryantii* are 50 nM by Lovley (1985) with strain M.o.H. and 16 nM by Conrad and Wetter (1990) with strain Bab 1. H_2 thresholds for a non-formate-utilizing methanogen, *Methanobacterium thermoautotrophicum*, are 85–95 nM by Lee and Zinder (1988) and 71 nM by Conrad and Wetter (1990).

In contrast to the previous studies, we report a much lower thermodynamic threshold for *M. bryantii* M.o.H. in DSMZ medium #119 for *M. bryantii* M.o.H. The differences between our threshold value and those from past studies may come from various reasons, e.g., different medium composition, mixing intensity, temperature, or utilization of simple organic compounds instead of or along with H_2 by the microorganisms other than *M. bryantii* M.o.H. However, a satisfactory explanation for differences between any pair of threshold values can only come from meticulous comparison of those individual studies and, perhaps, by conducting exactly the same experiments by both research groups.

Although we cannot explain the higher threshold valued obtained by other researchers, we obtained our threshold values with *M. byrantii* M.o.H., a strict H_2 oxidizer, repeatedly (21 times) for a large range of experimental conditions. Besides measuring H_2, we also measured CH_4 and biomass in the experiments, thereby providing a comprehensive and consistent picture of *M. bryantii* M.o.H. up to and after the H_2 thresholds.

Viewed in the light of our results, several previous studies reported a H_2 threshold for non-methanogenic microorganisms in the same range as ours. Experiments with *Paracoccus denitrificans*, a facultative Knallgas bacterium that can use H_2 as the electron donor and O_2 under aerobic and N_2O, NO_3^-, and NO_2^- under anaerobic conditions as the electron acceptors, gave H_2 threshold concentrations around 0.6 nM for all four acceptors (Häring and Conrad 1991). The computed strict-thermodynamic threshold is much smaller for H_2 oxidation with NO_3^-, in the range of 10^{-35} nM. Experiments with iron-reducing *Shewanella putrefaciens* (H_2 + Fe(III)) and nitrogen-fixing aerobic *Bradyrhizobium japonicum* ($H_2 + O_2$) gave similar threshold results, around 0.3 nM (Klüber and Conrad 1993), despite different strict-thermodynamic thresholds orders of magnitude lower, e.g., 10^{-11} nM for iron reduction. The observed H_2 thresholds for microbial reductions of nitrate, iron, and for reductive dehalogenation were around 0.1–0.4 nM in batch experiments (Lu et al. 2004), although standard free energies of these reactions vary significantly, i.e., –75 kJ/ mol-H_2 for sulfate reduction and –151 kJ/mol-H_2 for reductive dehalogenation of tetrachloroethene to trichloroethene. Similarly, H_2 thresholds were around 0.3 nM for sulfate reduction and reductive dehalogenation in sediment microcosm studies (Mazur and Jones 2001). Thus, our observed H_2 threshold value for *M. bryantii* M.o.H., around 0.4 nM, is consistent with what others observed for microorganisms using totally different electron acceptors. The fact that several other studies found a similar H_2 threshold suggests that a common control mechanism for H_2 oxidation might be central for a variety of aerobic and anaerobic microorganisms that oxidize H_2.

Our results are unique, however, because the final ΔG values for methanogenesis from H_2 included many positive values (Table 1). This finding requires that H_2 thresholds must be controlled by a reaction separate from the normal respiratory reaction. We explain our thresholds by *M. byrantii* removing electrons from H_2 and transferring them to solid biomass components. Since all microorganisms are made up of similar solid components, our explanation could hold for

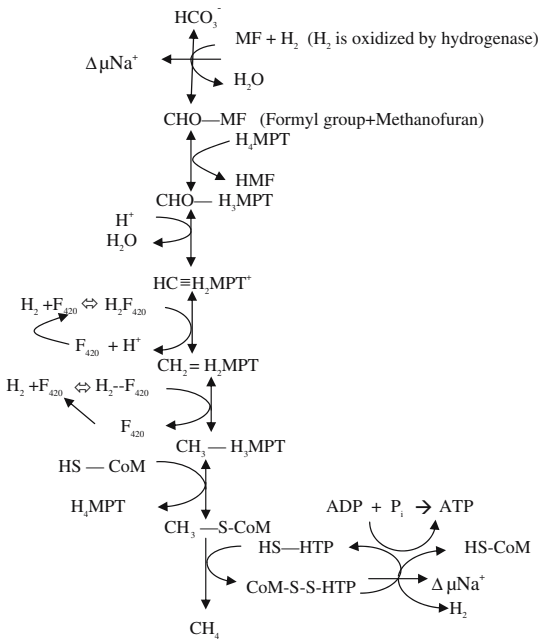

Fig. 7 Pathway for reduction of CO_2 to CH_4 in methanogens (adopted from Blaut et al. 1992). The steps from CO_2 to CH_3-S-CoM are reversible, but the last step is irreversible. In the last step, the methyl-Coenzyme M complex reacts with Coenzyme B (HS-HTP) to form CH_4 and heterodisulfide (CoM-S-S-HTP). ATP is generated via the proton motive force (PMF) during reduction of the heterodisulfide to coenzyme B and coenzyme M with electrons from oxidation of H_2

the observed thresholds of the other microorganisms, too.

Recent reviews of the biochemistry and enzymology of methanogenesis report that the last step of methane production is irreversible (Deppenmeier 2002; Thauer 1998; Peinemann et al. 1990). Figure 7 shows the biochemical pathway for reduction of CO_2 to CH_4 by methanogens. All the steps involved in reducing CO_2 to the methyl level are reversible reactions (Deppenmeier 2002; Thauer 1998). On the other hand, the last step of methanogenesis, the reduction of the methyl group in methyl-coenzyme M complex to methane, is irreversible (Thauer 1998). Methyl-coenzyme M and coenzyme B react to form methane and heterodisulfide, the step linked to ATP generation through proton motive force (Peinemann, et al. 1990; and our Fig. 7). Formation of methane is an irreversible ''one-way'' reaction that prevents methanogens from oxidizing CH_4 once it is formed (Thauer 1998; and our Fig. 5). It should be noted the methyl-Coenzyme-M from authentic methanogens is different than methyl-Coenzyme-M of methane-oxidizing bacteria by a new nickel protein that is similar to Cofactor F_{430} (Krüger et al. 2003); thus, authentic methanogens cannot oxidize methane. As further proof, *M. bryantii* M.o.H. did not oxidize CH_4 when provided with excess CH_4 and minimal H_2 in our experiments (Figs. 1, 2, 3, 5), but it produced H_2 from oxidation of biomass (Fig. 6).

Similarly, the last steps of other dissimilatory reactions also are irreversible: reduction of O_2 to H_2O catalyzed by complex IV (Nicholls and Ferguson 2002); reduction of NO_2^- to N_2O during denitrification, and potentially reduction of N_2O to N_2 (Zehnder 1988; Ye et al. 1994); reduction of sulfite to sulfide, thiosulfate, or trithionate in dissimilatory sulfate reduction (Zehnder 1988). The irreversibility of iron (Fe(III)) and manganese (Mn(IV)) reduction is not known (Straub et al. 2001). However, similarities between electron-transport chains of aerobic and anaerobic microorganisms suggest that the last step of iron and manganese reduction is also irreversible (Nicholls and Ferguson 2002). Irreversibility for the last step of respiration suggests a reason why microorganisms may divert electron flow away from the normal terminal electron acceptor when H_2 is present at a very low concentration. They may be able to obtain energy from H_2 oxidation or reduction, depending on the concentration of H_2, if all reactions involved in electron flow are reversible.

For methanogenesis (and, perhaps, other terminal electron accepting processes), the irreversible nature of the final end-product formation suggests why the concentration of this end product does not control the thermodynamics of H_2 oxidation near the H_2 threshold. Equilibrium thermodynamics, as described by the Gibbs free-energy relationship, are strictly accurate only for a reversible reaction (Stumm and Morgan 1996), but the final step is irreversible for normal respiration.

We observed that starved *M. bryantii* cells oxidized H_2, although they neither produced nor consumed CH_4 (Fig. 5). Previous studies showed that methanogens produce H_2 under low H_2

concentration (Valentine et al. 2000), and we also observed H_2 generation from *M. bryantii* without CH_4 production or consumption (Fig. 6). Thus, H_2 oxidation is a bidirectional reaction that occurs at several enzymatic centers in methanogens (Fig. 7). Consequently, equilibrium thermodynamics can be used to describe H_2 oxidation as long as electrons from H_2 oxidation are transferred to an electron acceptor that is linked by a reversible reaction. Because the thermodynamic threshold fell into a narrow range for our experiments and is similar to thresholds observed with other types of microorganisms, we hypothesize that the electron sink at the H_2 oxidation is a solid-phase cell component, which has an invariant activity of one in all cases.

Physiologically, the solid-phase component can be comprised of numerous proteins that are part of biomass. It need not be a particular compound or a storage material, as long as it is a solid. The validity of the solid-phase electron sink is supported by the results in Fig. 5, in which starved *M. bryantii* cells oxidized H_2 without producing methane, and in Fig. 6, in which rapidly growing *M. bryantii* generated H_2 and CH_4 when we stripped H_2 from the medium to make both reaction thermodynamically feasible.

An interesting observation about our H_2 threshold (~0.4 nM) is that it is close to the liquid-phase H_2 concentration in equilibrium with ambient atmospheric H_2 on Earth (also ~0.4 nM) (Manahan 1994). Perhaps the Earth's ambient H_2 concentration is controlled by a mechanism common to a large variety of microorganisms. Thus, the hypothesis of a solid-phase electron sink, coupled with the observations that many microbial types have a similar H_2 threshold, is consistent with a common mechanism that keeps the Earth's H_2 concentration near 0.4 nM.

Conclusions

We comprehensively evaluated H_2 thresholds for the obligate H_2-oxidizing methanogen *Methanobacterium bryantii* M.o.H. in light of microbial thermodynamic and kinetic principles. The thermodynamic H_2 threshold for *M. bryantii* M.o.H. was not controlled by ΔG for methane production from H_2. Instead, we repeatedly (21 times) attained a H_2 threshold near 0.4 nM, giving positive ΔG values for methanogenesis from $H_2 + HCO_3^-$, +5 to +7 kJ/mol-H_2, in most cases. Thus, the thermodynamics of methane production could not have controlled the H_2 threshold. Instead, we postulate that the H_2 threshold was controlled by a second reaction in which the electrons from H_2 oxidation are transferred to an electron sink that we hypothesize is a solid-phase component of the cells. We also show that a kinetic threshold (S_{min}), which is controlled by the rates of H_2 consumption and biomass growth, occurs at a H_2 concentration of about 2400 nM, at which biomass growth shifts from positive to negative.

Acknowledgments The authors thank Prof. David A. Stahl and Dr. Bradley E. Jackson for their invaluable comments and contributions at different stages of this research.

References

Benstead J, Archer DB, Lloyd D (1991) Formate utilization by members of the genus Methanobacterium. Arch Microbiol 156:34–37

Blaut M, Muller V, Gottschalk G (1992) Energetics of methanogenesis studied in vesicular systems. J Bioenerg Biomembr 24:529–546

Boone DR (1987) Replacement of the type strain of *Methanobacterium formicicum* and reinstatement of *Methanobacterium bryantii* sp. nov. nom. Rev. (ex Balch and Wolfe, 1981) with M.o.H. (DSM 863) as the type strain. Int J Syst Bacteriol 37:172–173

Boone DR, Mah R (1989) Methanogenic archeobacteria. In: Murray RGE, Holt JG, Staley JT, Pfenning N (Eds) Bergey's manual of systematic bacteriology. Williams & Wilkins, Baltimore, pp 2175–2177

Brown DG, Komlos J, Jaffé P (2005) Simultaneous utilization of acetate and hydrogen by Geobacter sulfurreducen and implications for use of hydrogen as an indicator of redox conditions. Environ Sci Technol 39:3069–3076

Chapelle FH, Haack SK, Adriaens P, Henry MA, Bradley PM (1996) Comparison of E_h and H_2 measurements for delineating redox processes in a contaminated aquifer. Environ Sci Technol 30:3565–3569

Conrad R, Aragno M, Seiler W (1983) The inability of hydrogen bacteria to utilize atmospheric H_2 is due to threshold and affinity for hydrogen. FEMS Microbiol Lett 18:207–210

Conrad R, Wetter B (1990) Influence of temperature on energetics of hydrogen metabolism in homoacetogenic, methanogenic, and other anaerobic bacteria. Arch Microbiol 155:94–98

Conrad R (1996) Soil microorganisms as controllers of atmospheric trace gases (H_2, CO_2, CH_4, OCS, N_2O, and NO). Microbiol Rev 60:609–640

Cord-Ruwisch R, Seitz H-J, Conrad R (1988) The capacity of hydrogenotrophic anaerobic bacteria to compete for traces of hydrogen depends on the redox potential of the terminal electron acceptor. Arch Microbiol 149:350–357

Deppenmeier U (2002) The unique biochemistry of methanogenesis. Prog Nucleic Acid Res Mol Biol 71:223–283

Deutsche Sammlung von Mikroorganismen und ZellKulturen GmbH. http://www.dsmz.de or http://www2.dsmz.de

Dolfing J, Janssen DB (1994) Estimates of Gibbs free energies of formation of chlorinated aliphatic compounds. Biodegredation 5:21–28

Häring V, Conrad R (1991) Kinetics of H_2 oxidation in respiring and denitrifying *Paracoccus denitrificans*. FEMS Microbiol Lett 78:259–264

Hoehler TM, Alperin MJ, Albert DB, Martens CS (1998) Thermodynamic control on hydrogen concentrations in anoxic sediments. Geochim Cosmochim Acta 62:1745–1756

Jackson BE, McInerney MJ (2001) Anaerobic microbial metabolism can proceed close to thermodynamic limits. Nature 415:454–456

Karadagli F, Rittmann BE (2005) Kinetic characterization of *Methanobacterium bryantii* M.o.H. Environ Sci Technol 39:4900–4905

Kassenga G, Pardue JH, Moe WM et al (2004) Hydrogen thresholds as indicators of dehalorespiration in constructed treatment wetlands. Environ Sci and Technol 38:1024–1030

Klüber HD, Conrad R (1993) Ferric iron-reducing *Shewanella putrifaciens* and N_2-fixing *Bradyrhizobium japonicum* with uptake hydrogenase are unable to oxidize atmospheric H_2. FEMS Microbiol Lett 111:337–342

Kotsyurbenko OR, Glagolev MV, Nozhevnikova AN, Conrad R (2001) Competition between homoacetogenic bacteria and methanogenic archea for hydrogen at low temperature. FEMS Microbiol Ecol 38:153–159

Krumholz LR, Harris SH, Tay ST, Suflita JM (1999) Characterization of two subsurface H_2-utilizing bacteria, *Desulfomicrobium hypogenium* sp. nov. and *Acetobacterium psammolithicum* sp. nov., and their ecological roles. Appl Environ Microbiol 65: 2300–2306

Krüger M, Meyerdierks A, Gröckner FO, Amann R, Widdel F et al (2003) A conspicous nickel protein in microbial mats that oxidize methane anaerobically. Nature 426:878–881

Lee MJ, Zinder SH (1988) Hydrogen partial pressures in a thermophilic acetate-oxidizing methanogenic coculture. Appl Environ Microbiol 54:1457–1461

Ljungdahl LG, Wiegel J (1986) Working with anaerobic bacteria. In: Demain AL, Solomon NA (Eds) Manual of industrial microbiology and biotechnology. Amer. Soc. Microbiol., Washington, D.C., pp 84–96

Lovley DR, Dwyer DF, Klug MJ (1982) Sulfate reducers can outcompete methanogens at freshwater sulfate concentrations. Appl Environ Microbiol 43:1373–1379

Lovley DR, Klug MJ (1983) Kinetic analysis of competition between sulfate reducers and methanogens for hydrogen in sediments. Appl Environ Microbiol 43:187–192

Lovley DR (1985) Minimum threshold for hydrogen metabolism in Methanogenic Bacteria. Appl Environ Microbiol 49:1530–1531

Lovley DR, Goodwin ST (1988) Hydrogen concentrations as an indicator of the predominant terminal electron-accepting reactions in aquatic sediments. Geochim Cosmochim Acta 52:2993–3003

Lovley DR, Chapelle FH, Woodward JC (1994) Use of dissolved H_2 concentrations to determine distribution of microbially catalyzed redox reactions in anoxic groundwater. Environ Sci Technol 28:1205–1210

Löffler FE, Champine JM, Ritalahti KM, Sprague SJ, Tiedje JM (1997) Complete reductive dechlorination of 1,2-Dichlorpropane by anaerobic bacteria. Appl Environ Microbiol 63:2870–2875

Löffler FE, Tiedje JM, Sanford RA (1999) Fraction of electrons consumed in electron acceptor reduction and hydrogen threshold as indicators of halorespiratory physiology. Appl Environ Microbiol 65:1373–1379

Lu XX, Tao S, Bosma T, Gerritse J (2004) Characteristic hydrogen concentrations for various redox processes in batch study. J Environ Sci Health Part A 36:1725–1734

Luijten MLGC, Roelofsen W, Langenhoff AAM, Schraa G, Stams AJM (2004) Hydrogen threshold concentrations in pure cultures of halorespiring bacteria and at site polluted with chlorinated ethenes. Environ Microbiol 6:646–650

Mägli A, Martingo FA, Leisinger T (1995) Acetogenesis from dichloromethane by a two-component mixed culture comprising a novel bacterium. Appl Environ Microbiol 61:2943–2949

Manahan SE (1994) Environmental chemistry, 6th edn. Lewis Publishers, Boca Raton, Florida

Mazur CS, Jones WJ (2001) Hydrogen concentrations in sulfate-reducing estuarine sediments during PCE dehalogenation. Environ Sci Technol 35:4783–4788

Monod J (1949) The growth of bacterial cultures. Annu Rev Microbiol 3:371–394

Namkung E, Rittmann BE (1987) Evaluation of bisubstrate secondary utilization kinetics by biofilms. Biotechnol and Bioengin 29:335–342

Nicholls DG, Ferguson SJ (2002) Bioenergetics 3. Academic Press, London

Peinemann S, Hedderich R, Blaut M, Thauer R, Gottschalk G (1990) ATP synthesis coupled to electron transfer from H_2 to the heterodisulfide of 2-mercaptoethanosulfonate and 7-mercaptoheptanoylthreonine phosphate in vesicle preparations of the methanogenic bacterium strain Gö1. FEBS Lett 263:57–60

Rittmann BE, McCarty PL (1980a) Model of steady-state-biofilm kinetics. Biotech Bioeng 22:2343–2357

Rittmann BE, McCarty PL (1980b) Model of steady-state-biofilm kinetics. Biotech Bioeng 22:2359–2373

Rittmann BE, McCarty PL (2001) Environmental biotechnology: Principles and applications. McGraw-Hill, New York

Robinson JA, Tiedje JM (1984) Competition between sulfate-reducing and methanogenic bacteria for H_2 under resting and growing conditions. Arch Microbiol 137:26–32

Schink B (1997) Energetics of syntrophic cooperation in methanogenic degradation. Microbiol Mol Biol Rev 61:262–280

Seitz H-J, Schink B, Conrad R (1988) Thermodynamics of hydrogen metabolism in methanogenic cocultures degrading ethanol and lactate. FEMS Microbiol Lett 55:119–124

Shrout JD, Scheetz TE, Casavant TL et al (2005) Isolation and characterization of autotrophic, hydrogen-utilizing, perchlorate-reducing bacteria. App Microbiol Biotech 67:261–268

Straub KL, Benz M, Schink B (2001) Iron metabolism in anoxic environments at near neutral pH. FEMS Microbiol Ecol 34:181–186

Stumm W, Morgan JJ (1996) Aquatic chemistry: Chemical equilibria and rates in natural waters, 3rd edn. John-Wiley and Sons, Inc., New York

Thauer RK (1998) Biochemistry of methanogenesis: a tribute to Marjory Stephenson. Microbiology 144:2377–2406

Tiedje JM (1988) Ecology of denitirification and dissimilatory nitrate reduction to ammonium. In: Zehnder AJB (Eds) Biology of anaerobic organisms. John-Wiley and Sons, Inc., New York, pp 179–244

Valentine DL, Blanton DC, Reeburgh WS (2000) Hydrogen production by methanogens under low-hydrogen conditions. Arch Microbiol 174:415–421

Widdel F (1988) Microbiology and ecology of sulfate- and sulfur-reducing bacteria. In: Zehnder AJB (Eds) Biology of anaerobic organisms. John-Wiley and Sons, Inc., New York, pp 469–585

Yang Y, McCarty PL (1998) Competition for hydrogen within a chlorinated solvent dehalogenating anaerobic mixed culture. Environ Sci Technol 32:3591–3597

Ye RW, Averill BA, Tiedje JM (1994) Denitrification: production and consumption of nitric oxide. Appl Environ Microbiol 60:1053–1058

Zinder SH (1993) Physiological ecology of methanogens. In: Ferry JG (Eds) Methanogenesis: Ecology, pysiology, biochemistry, and genetics. Chapman and Hall, Inc., New York, pp 128–206

Zehnder AJB (ed) (1988) Biology of anaerobic microorganisms. John Wiley & Sons, New York